Electrical characterization of thin film ferroelectric capacitors

M. P. J. Tiggelman, K. Reimann, M. Klee, D. Beelen, W. Keur, J. Schmitz, and R. J. E. Hueting

***Abstract*— Tunable capacitors can be used to facilitate the reduction of components in wireless technologies. The tunability of the capacitors is caused by the sensitivity of the relative dielectric constant to a change in polarization with electric field. Thin film ferroelectric MIM capacitors on silicon offer a re-use of electronic circuitry, low tuning voltages, a high capacitance density, a low cost, a presence of bulk acoustic wave resonance(s) and decoupling functionality. The basic operation and measurement principles are outlined. To assess the performance in the microwave frequency range, MIM test structures[1], with a barium strontium titanate dielectric, have been successfully processed, and measured. The electrical characterization of tunable capacitors is demonstrated using a 1-Port Advantest R3767CG VNA in the frequency range of 10 MHz – 8 GHz.**

***Index Terms*— ferroelectric, MIM, tunable capacitor, barium strontium titanate, and high-k dielectric.**

I. Introduction

Developments in solid-state ferroelectrics suited for microwave applications are an on-going research effort for more than 30 years [1]. Ferroelectric material is often integrated in capacitor structures. Integration of these electronic building blocks on silicon has numerous advantages:

1) continuous (low voltage) tuning,
2) low cost,
3) high capacitance density due to the high-κ material and thin film technology, and
4) decoupling.

The applicability of these types of capacitors has been pointed out in literature by typical applications such as phased shifters [2], impedance matching networks [3], delay lines [4], or tunable filters [5].

The industry has been focusing on different ferroelectric materials. The most frequently used ferroelectric is barium strontium titanate $(Ba,Sr)TiO_3$. To assess the performance of the metal-insulator-metal (MIM) test structures electrical characterization is performed.

In this work the electrical characterization of ferroelectric capacitors is successfully demonstrated. The basics of the ferroelectric material, the test structures, and typical measurement results are discussed from f = 10 MHz – 8 GHz using an Advantest R3767CG vector network analyzer (VNA) with a 1-Port configuration.

II. Basic operation

A tunable capacitor with a $(Ba,Sr)TiO_3$ dielectric can operate typically in two phase regions. The operating region depends on the temperature, and the composition of the ferroelectric material. The effect on the relative dielectric constant is indicated in fig. 1.

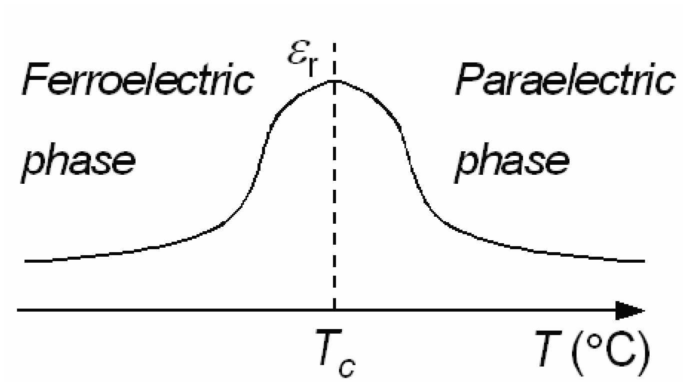

Fig.1 The relative dielectric constant ε_r of the ferroelectric material with temperature.

The Curie temperature T_c separates the phase regions, and indicates the maximum relative dielectric constant ε_r at zero DC voltage with a symmetrical stack. The differences between the phase regions are indicated in table 1.

	Ferroelectric phase	Paraelectric phase
Temperature T	$T < T_c$	$T > T_c$
Crystal structure	Tetragonal	Cubic
Loss tangent tanδ	Higher	High
Tunability n	Higher	High

Table 1. Basic modes of operation of a ferroelectric $(Ba,Sr)TiO_3$ material.

Manuscript received September 27th 2006. This work was supported by NXP (former Philips Semiconductors), and the University of Twente.

M. P. J. Tiggelman is a PhD student from the MESA+ Institue for Nano Technology working at NXP in Eindhoven (corresponding author to provide phone: +31 (0)40-2746247; fax: +31 (0)40-2743352; e-mail: nlv14139@natlab.research.philips.com).

The latter two points in the table are known as the performance parameters of a tunable capacitor. The tunability *n*, expressed in eq.1, defines the amount of capacitance tuning from zero DC voltage until a specific voltage (lower than the breakdown voltage).

$$\text{Tunability } n = \frac{\varepsilon_r(0\,V_{dc}) - \varepsilon_r(V\max)}{\varepsilon_r(0\,V_{dc})} \qquad (1)$$

The loss tangent, expressed in eq. 2, indicates of the intrinsic loss in the ferroelectric material and the electrodes.

$$\text{Loss tangent } \tan\delta = \frac{\Re(Z_{11})}{|\Im(Z_{11})|} \qquad (2)$$

The combination of these factors can give a quick performance assessment of the capacitor. For microwave applications the general requirements are a low loss tangent and a high tunability. The loss tangent is higher in the ferroelectric phase due to hysteresis effects caused by spontaneous polarization. The contribution of ferroelectric domains causes extra losses compared to test structures operating in the paraelectric phase region [6]. A DC bias saturates the polarization in reducing the relative dielectric constant (see figure 9).
Since measurements are performed from 1 kHz up to the 1 MHz with an impedance/gain-phase analyzer the focus in this article will be on the effects of applying a DC bias in a wider frequency range with a VNA.

III. RF MEASUREMENT SETUP AND PARAMETERS

The performance assessment of the tunable capacitors is performed with a typical 1-Port RF measurement setup as shown in fig. 2.

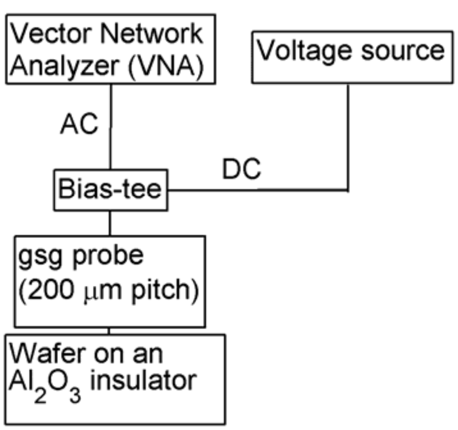

Fig.2 A 1-Port S_{11}-parameter RF measurement setup.

The magnitude and phase information of the 1-Port measurement data are contained in the insertion loss s_{11}-parameter output of the VNA. A Matlab program converts the s_{11}-parameters to impedance Z_{11}-parameters. A simple equivalent model, shown in fig.3, represents the tunable capacitor, and can be used for electrical characterization. This model can be converted to *Z*-parameters. From this point forward the frequency and voltage behavior of the relative dielectric constant ε_r, the capacitance C_s, the tunability *n* expressed in eq.1, loss tangent tanδ expressed in eq. ~~3~~2, and the the series resistance R_s, can be determined.

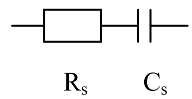

Fig.3 The equivalent series R_s-C_s model of a tunable ferroelectric capacitor.

The relative dielectric constant ε_r can be expressed as

$$\varepsilon_r = \frac{C_s \cdot d}{\varepsilon_0 \cdot A}\ , \qquad (3)$$

whereby the free permittivity of free space ε_0 = 8.85e-12 F/m, the area *A*, and the dielectric thickness *d*.

From the ε_r(V) curve information can be obtained e.g. hysteresis effects, capacitor symmetry, proper grounding, and the breakdown voltage. The two main performance parameters, the tunability and loss tangent, are expressed in eq.1 and 2.

IV. RF TEST STRUCTURES

The layout of the test structures is based on a technique described by Ma et al.[7]. Only the top electrode is structured for the capacitor design (see fig.4). The RF test structures are designed for GS or GSG RF probes.

Cross view: Top view

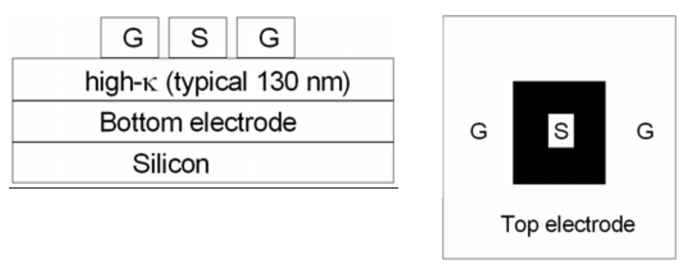

Fig.4 The upper picture displays the cross view, and the lower placed figure displays the top view of the RF test structures.

A large capacitance goes from the ground top electrode to the bottom electrode, and a small capacitance from the signal electrode to the bottom electrode. The total capacitance resembles two capacitors in series. The total capacitance equals the small capacitance from the top signal electrode to the bottom electrode.

V. MEASUREMENT RESULTS

The scatter parameter s_{11} of a wide-band VNA can be transformed to give valuable characteristics about the frequency dependency of the tunable MIM capacitors. The measurements are performed from f = 10 MHz until f = 8 GHz. The previously mentioned parameters are investigated further.

<u>The relative dielectric constant ε_r</u>

In the frequency range of several MHz up to several hundred MHz the relative dielectric constant ε_r is nearly constant (see fig.5) as one would expect. Another observation is that the ε_r decreases with a higher field as explained briefly in section II.

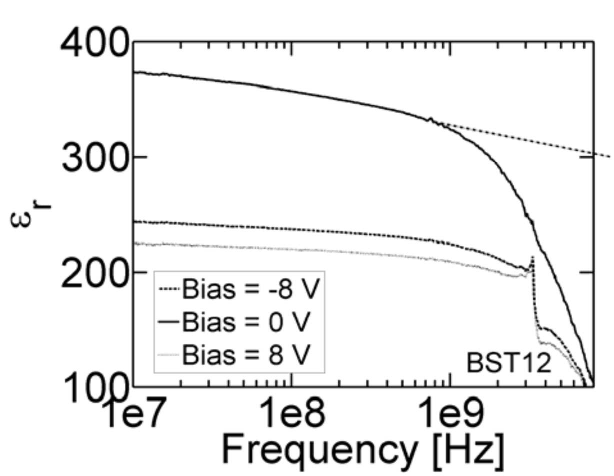

Fig.5 The relative dielectric constant with frequency of a thin film (dielectric thickness *d* = 273 nm) capacitor with a size of 50 μm x 50 μm at room temperature.

At high radio frequencies the series resistance of the electrodes can become the limiting performance factor. This will be elaborated further in the figure with the real part of the impedance $\Re(Z_{11})$ with frequency.

If the frequency exceeds $f \geq 1$ GHz from the relaxation behavior (straight dash-dotted line) then the ε_r(f) deviates. The lumped capacitor becomes distributed if the fields change considerably by within the dimension of the test structure. The charge is concentrated around the probe-tip reducing the effective area, and thereby the relative dielectric constant. The capacitor must then be described as a distributed RC network (see fig. 6). At f = 3 GHz the electrostrictive dielectric material [8] causes a bulk acoustic resonance with applied bias.

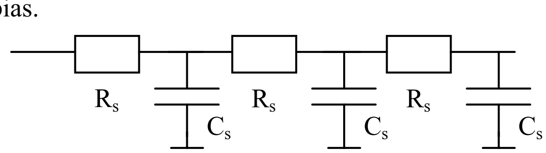

Fig.6 A distributed RC network.

<u>The series capacitance C_s</u>

The series capacitance is proportional to the relative dielectric constant, and is expressed in eq. 3.

<u>The tunability *n*</u>

The tunability performance parameter in fig. 7 follows from the measurement data in fig. 5. The minimum (-20 V) and maximum breakdown voltage (24 V) are incorporated in the tunability figure.

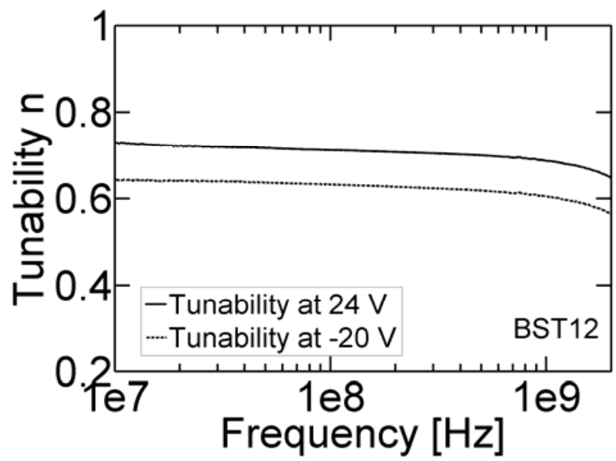

Fig. 7 The frequency dependency of the tunability *n* shows an excellent tuning range for both the minimum and maximum DC voltage.

Both curves show an excellent tuning range for both the negative and positive DC voltage.

<u>The loss tangent tanδ</u>

The second performance parameter, the loss tangent tanδ, is the sum of the high-κ material loss and the electrode series resistance loss. At low frequencies and high fields the leakage current dominates and at higher frequencies the electrode resistance determines the performance of the thin film high density (tunable) capacitor [9]. The left side of the minimum loss tangent in fig. 8 indicates the dielectric loss, and the loss on the right side is dominated by the thickness and conductivity of the bottom and top electrode. The intrinsic loss tangent of the material is not visible yet. It should be a plateau between the two other regimes. The leakage current dominates the loss below f = 4 MHz. At 0 V bias the dielectric loss become visible at high voltages. However, the constant

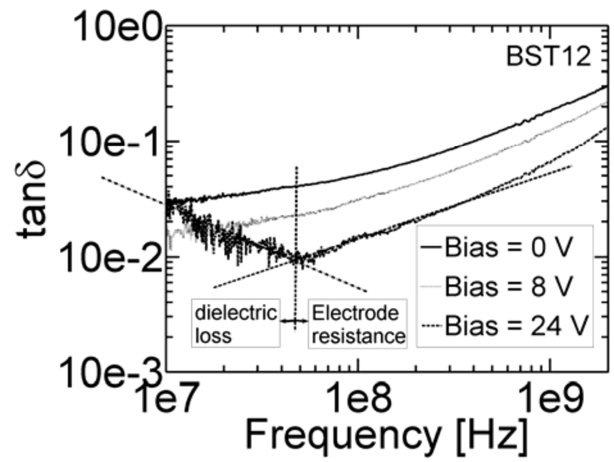

Fig.8 The loss tangent vs. frequency at different voltages until breakdown.

series resistance contribution of the electrodes dominates the loss at radio frequencies (see the linear dotted slope at the right side of the optimum). The loss tangent can be modeled by means of the series model. The loss tangent can be expressed by

$$\tan\delta = \frac{\Re(Z_{11})}{|\Im(Z_{11})|} = \omega R_s C_s \quad (4)$$

This formula indicates that the loss tangent will decrease if the series capacitance becomes less by e.g. applying a bias or by using smaller capacitors.

Series resistance $\Re(Z_{11})$

The series resistance is equal to the real part of the impedance (see the series model in fig. 3). At higher frequencies the real part becomes constant (see fig. 9) and is equal to the effective electrode resistance.

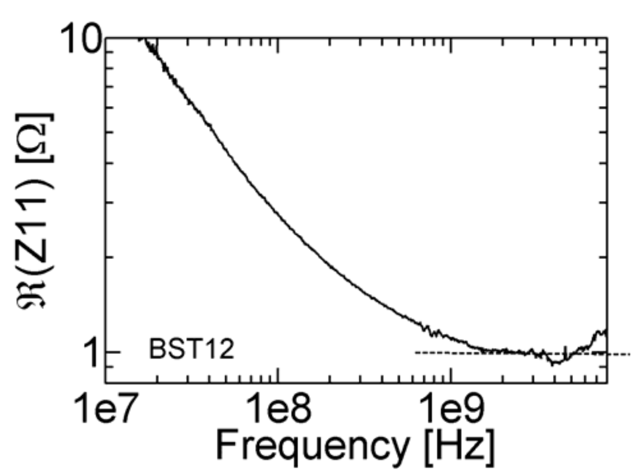

Fig.9 The real part of the impedance $\Re(Z_{11})$.

The series resistance contribution at RF is proportional to the sheet resistance of the electrodes. The series capacitance and the series resistance are quite constant at RF. The eq.4 of the loss tangent is capable of predicting the behavior of the loss tangent at RF.

Capacitance-voltage curve

A typical C_s-V_{dc} is measured from zero DC voltage in steps of 2 V until breakdown at both sides with the VNA and a DC voltage source.

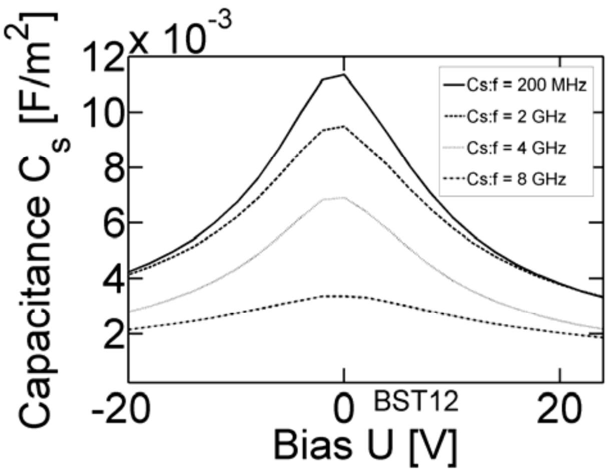

Fig. 10 The C_s-V_{dc} curve of two test structures with identical shape and dimensions at different frequencies.

The C_s-V_{dc} curve in fig. 10 is almost symmetric for positive and negative voltages. The capacitance and tunability decrease with frequency in the RF range due to distributed effects as explained earlier.

VI. CONCLUSIONS

The electrical characterization of tunable ferroelectric capacitors with a VNA has successfully been demonstrated. An excellent tuning range and low intrinsic dielectric losses have been obtained. Smaller test structures with better conducting electrodes will improve performance at RF.

ACKNOWLEDGEMENTS

The author would like to thank M. Ruediger of Philips Research for manufacturing part of the samples.

REFERENCES

[1] K. Bethe, *"Uber das mikrowellenverhalten nichlinearer dielektrika"*, Philips Research Report, Vol. 25, Suppl.2, 1970

[2] Q. Meng et al., *"An impedance matched phase shifter using BST thin film"*, IEEE Microwave and wireless components letters, vol 16, no. 6, June 2006.

[3] L.-Y. Vicki Chen, Roger Forse, D. Chase, and Robert A. York, *"Analog Tunable Matching Network Using Integrated Thin-Film BST Capacitors"*,IEEE MTT-S Digest, 2004.
[4] D. Kuylenstierna, A. Vorobiev, P. Linnér, and S. Gevorgian, *"Ferroelectrically Tuneable Delay Lines"*, 34th European Microwave Conference, 2004.
[5] J. Nath et al, *"An Electronically Tunable Microstrip Bandpass Filter Using Thin-Film Barium–Strontium–Titanate (BST) Varactors"*, IEEE Transactions on microwave theory and techniques, vol. 53, no. 9, September 2005.
[6] A.K. Tagantsev, V.O. Sherman, K.F. Astafiev, J. Venkatesh & N. Setter, *"Ferroelectric Materials for Microwave Tunable Applications"*, Journal of Electroceramics, vol. 11, pp. 5–66, 2003.
[7] Z. Ma et al., *"RF Measurement Technique for Characterizing Thin Dielectric Films"*, IEEE Transactions on electron devices, vol. 45, no. 8, August 1998.
[8] W.P. Mason, "Electrostrictive effect in Barium Titanate Ceramics", Physical Review, vol. 74, no.9, November 1948.
[9] J. Schmitz, F. N. Cubaynes, R. J. Havens, R. de Kort, A. J. Scholten, and L. F. Tiemeijer, *RF Capacitance–Voltage Characterization of MOSFETs With High Leakage Dielectrics",* IEEE Electron Devices Letters, vol. 24, no.1, January 2003.